Fluorescence Study for the Electrostatic Interaction and Aggregation in Dilute Polar Solution of Polyelectrolytes

*Qilong SUN, Biye REN, Xinxing LIU, Fang ZENG, Ping LIU, Zhen TONG**

Research Institute of Materials Science, South China University of Technology, Guangzhou 510640, China

Summary: Fluorescence decay and quenching of pyrene labels on copolymers of 2-acrylamido-2-methylpropanesulphonic acid (AMPS) and *N*,*N*-dimethylacrylamide (DMAA) were observed in dilute salt-free aqueous solutions as a function of the mole fraction F_{AMPS} of AMPS from 0 to 0.896. Monoexponential and biexponential decays were found for the samples of $F_{AMPS} < 0.35$ and samples of $F_{AMPS} > 0.35$, respectively. The fast decay component is 80% and the averaged lifetime $<\tau>$ and lifetime τ_1 of the fast decay decreased with increasing F_{AMPS}. Quenching efficiency of Cu^{2+}, CH_3NO_2, and dinitrobenzene to the pyrene label was investigated in the framework of Stern-Volmer plot. The quenching effects of Cu^{2+} included both of dynamic and static ones, the latter was due to the condensed Cu^{2+}. For the neutral quenchers, the quenching rate constant k_q increased when $F_{AMPS} < 0.449$ then decreased, showing a decline of accessibility to the pyrene label. I_1/I_3 value in salt-free dilute aqueous solution and in DMSO solution decreased obviously with an increase in F_{AMPS}, indicating that the labeled fluorophore experienced a decrease in polarity of its microenvironment with increasing charge density of the polymer. This I_1/I_3 decrease was enhanced with increasing the polymer concentration and adding salt NaCl up to 0.75 mol/L showed no effect on the appearance of this decrease. These results were interpreted consistently with the counterion condensation concept, where condensed counterions induced the "temporal" aggregation of less-polar in the polyelectrolyte solutions surrounding the pyrene labels.

Introduction

Polyelectrolyte attracts researches for more than a half century due to its significance in many industrial areas and in modeling the assembly structure of DNA and proteins. According to the traditional consideration for polyelectrolytes in dilute aqueous solutions, the ionizable residues on the polymer will dissociate into polyions and counterions. The dominant interaction governing the molecular behavior of polyelectrolytes is the electrostatic repulsion screened by the atmosphere of small ions.[1, 2]

Actually, for a vinyl polymer with a pendant ionizable group on each repeat unit, the linear distance between two neighboring ions on the chain is about 2.5 Å, independent of polymer

 CCC 1022-1360/00/$ 17,50+.50/0

concentration when the polyelectrolyte is completely dissociated. This charge density is even higher than that in 10 mol/L of aqueous NaCl solution if it exists actually, leading to an unstable system due to the high free energy. This means that there is no infinite dilute state for polyelectrolytes as the reference state used for normal solutions and that the effective charge density should be reduced to decrease the electrostatic free energy. Based on this consideration, Oosawa[3] and Manning[4] proposed the counterion condensation concept. When the linear charge density of polyelectrolyte is beyond a threshold value, the counterion will condense surrounding the polyion to reduce the actual charge density. Then, the condensed counterions may cause a new kind of aggregation domain in the solution as suggested by the simulation of Ray and Manning.[5-8]

On the other hand, there exist abnormal observations for the structure of polyelectrolyte in polar solutions at low ionic strength. One example is the existence of fast and slow diffusion modes revealed by dynamic light scattering.[9-14] The origin of this slow mode, usually attributed to so-called large-scale "heterogeneities" or "domains" in the solution, is still unclear. Another example is the appearance of a peak in the angular dependence of the scattered intensity along with a steep upturn at very low scattering angles as observed by small angle neutron and X-ray scattering on polyelectrolyte solutions at low ionic strength.[12, 15, 16] This unusual scattering is electrostatic nature and corresponds to "multichain" domains. These observations seem to suggest the possible existence of somewhat aggregated structure in polar solutions of polyelectrolytes at low ionic strength.

Fluorescence is a powerful tool to monitor the change in the microenvironment surrounding the chromophore in polymer solutions.[17, 18] The fluorophore covalently attached to polymer chains can directly reflect the local situation of labeled polymer, such as local polarity, local viscosity, local segment mobility, and accessibility of the label. Therefore, pyrene labeled strong electrolyte copolymers of 2-acrylamido-2-methylpropanesulphonic acid (AMPS) and *N*,*N*-dimethylacrylamide (DMAA) were chosen because the homopolymers of AMPS and DMAA were completely dissolvable in water. The pyrene content in the polymer has to be restricted as low as 0.1 mol% to avoid the association induced by the aggregated labels.

Experimental Section

Synthesis of pyrene labeled sulfonate polyelectrolyte samples has been described elsewhere[19] and a brief introduction is given below. Pyrene label monomer *N*-(1-pyrenylmethyl)-methacrylamide (PyMA) was prepared from 1-pyrenylmethylamine hydrochloride (Aldrich)

according to the method of Ref. 20. 2-Acrylamido-2-methylpropanesulphonic acid (AMPS, Fluka), *N*,*N*-dimethylacrylamide (DMAA, Kohjin, Japan), and PyMA were initiated to copolymerize in DMSO/water mixture (2:3 in volume) at 70 °C by 0.2 mol% of ammonium persulfate. The total monomer concentration and PyMA content were kept at 0.80 mol/L and 0.1 mol%, respectively, while the monomer ratio of AMPS was changed to produce a series of samples with different charge densities. The refined products were analyzed with a Heraeus CHN-O apparatus and the F_{AMPS} value of AMPS mole fraction in the sample was evaluated. The weight averaged molecular weight M_w of samples was determined by gel permeation chromatography (GPC) of Waters using aqueous Na_2SO_4 solution of 0.1 mol/L as the eluent and poly(ethylene oxide) as the standard. The pyrene label content of 0.1 mol% in the sample was confirmed by UV absorbance. These samples were referred to as ADPy-x series; with x denoting the mole ratio of the AMPS monomer in the feed, and the composition and M_w are listed in Table 1.

Fluorescence lifetime was determined with a Horiba NABS-1100 time-resolved spectro-fluoremeter excited at 340 nm. The aqueous solution with polymer concentration c_P = 0.05 g/L was prepared by dissolving the ADPy sample in highly pure water (resistance of 18×10^6 Ωcm by a Millipore purification apparatus) for one day with stirring. Before measurement, the solution was deaerated by bubbling with highly pure nitrogen for 30 min.

Table 1. Composition of ADPy samples*

Sample	AMPS/DMAA in feed (mol)	yield (wt%)	F_{AMPS}	$M_w\times10^{-4}$	M_w/M_n
ADPy-0	0/100	78.55	0	-	-
ADPy-1	1/99	66.52	0.033	187	6.0
ADPy-5	5/95	80.95	0.147	72.2	4.8
ADPy-10	10/90	84.71	0.301	-	-
ADPy-20	20/80	63.31	0.449	40.1	3.1
ADPy-30	30/70	68.62	0.574	55.2	2.9
ADPy-45	45/55	84.58	0.711	84.1	2.6
ADPy-60	60/40	86.91	0.820	85.7	2.9
ADPy-75	75/25	89.50	0.896	80.8	2.8

*: Pyrene content is 0.1 mol% of total monomers.

The steady-state fluorescence emission spectrum was measured with a Hitachi F-4500 fluorescence spectrophotometer at 25 °C. The excitation wavelength was 343 nm with the

exciting and emitting slit of 5.0 and 2.5 nm, respectively, which were required because of low emission intensity due to very low label content in the samples. For the quenching experiments, the quencher solution of nitromethane in water (0.6 mol/L) or dinitrobenzene in ethanol (0.1 mol/L) was added into the polymer solution with a microsyringe. The aqueous quencher solution of cupric sulfate (0.02 mol/L) was mixed with a polymer solution first and then diluted to desired concentrations.

Results

Fluorescence Decay

Figure 1 shows experimental fluorescence decay data (points) of pyrene labels on five ADPy samples in water at concentration of c_P = 0.05 g/L. The decay is biexponential of the form[21]

$$I(t) / I(0) = \alpha_1 \exp(-t/\tau_1) + \alpha_2 \exp(-t/\tau_2) \qquad (1)$$

where $I(t)$ and $I(0)$ are the fluorescence intensities at time t and $t = 0$, respectively, α_i is the fraction of decay with the lifetime τ_i, and $\alpha_1 + \alpha_2 = 1$. The solid curves are the fit of eq (1) to the observed data, giving the parameters in Table 2. The monoexponential decay is observed for the samples ADPy-5 and ADPy-10 with lower F_{AMPS}, but the biexponential decay is the case for the other samples with higher F_{AMPS}. In the latter case, as F_{AMPS} is increased the lifetime τ_1 of the faster decay becomes shorter with constant α_1 and τ_2.

The biexponential decay of fluorescence emission has been found from aqueous solution of polyelectrolytes. Hoyle et al. considered a dual environment for pyrene probes in water-soluble polyphosphazene based on the biexponential decay.[22] Morishima and colleagues observed the biexponential decay of pyrene labels on polyelectrolytes with long alkyl side chains for

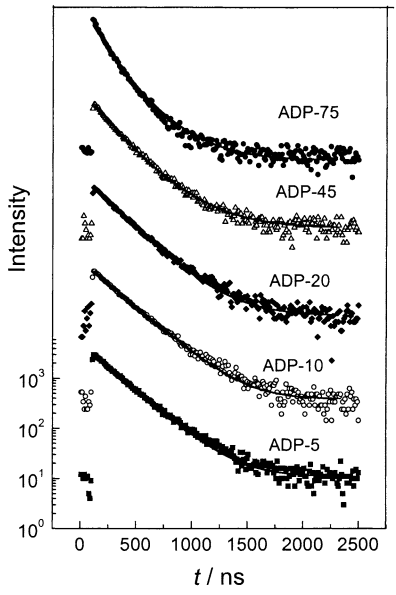

Figure 1. Fluorescence decay traces (points) of pyrene labels on indicated ADPy samples in aqueous solution at 25 °C with polymer concentration c_P of 0.05 g/L, the solid curves are the exponential fit with the parameters in Table 2.

hydrophobic modification and correlated the fraction of slower decay component with the mole fraction of hydrophobic modifier.[23, 24]

Table 2. Fluorescence lifetime of pyrene label on ADP in water solutions

Sample	F_{AMPS}	ξ	α_1	τ_1 /ns	τ_2 /ns	$<\tau>$* /ns	for Cu^{2+} quenching		
							K_{SV} /$Lmol^{-1}$	**K**	α
ADPy-5	0.147	0.420	1.0	231	-	231	100	80	0
ADPy-10	0.301	0.860	1.0	231	-	231	-	-	-
ADPy-20	0.449	1.283	0.8	180	290	202	700	80	0.0008
ADPy-45	0.711	2.031	0.8	145	290	174	1450	80	0.0008
ADPy-75	0.896	2.560	0.8	135	290	166	1700	80	0.0008

*$<\tau>$: Average lifetime, $<\tau> = \alpha_1\tau_1 + \alpha_2\tau_2$

The present results seem to suggest that there would be two different microenvironments for pyrene labels on the strong polyelectrolyte in aqueous solution when its charge density is beyond a specific value. One is more exposed to water and its lifetime becomes shorter from 231 ns with increasing charge density and the other is protected from water with the constant lifetime (290 ns) longer than 231 ns for the samples with lower charge density. Because of low pyrene content in polymers (0.1 mol%) and high solubility of homopolymers of AMPS and DMAA, these two different microenvironments appear to be the contribution of electrostatic interaction in the salt-free aqueous solution. However, the averaged lifetime $<\tau>$ decreases with increasing charge density because the whole polyelectrolyte chain becomes more extended, resulting in an obvious reduction of pyrene label's lifetime.

Fluorescence Quenching

The existence of different microenvironments for pyrene labels on polymers can be detected by the variation in their accessibility to fluorescence quencher. We quenched the fluorescence emission by various quenchers of cation Cu^{2+}, neutral nitromethane, and more hydrophobic neutral dinitrobenzene. The data were dealt with in the framework of Stern-Volmer plot as[25]

$$I_0/I = 1 + k_q \tau_0 [Q] \qquad (2)$$

where I_0 and I are the emission intensity at about 397 nm without quencher and with quencher, respectively; k_q is the quenching rate constant, τ_0 is the fluorescence lifetime without quencher ($<\tau>$ in Table 2 was used in evaluating k_q), and [Q] is the quencher concentration. The Stern-Volmer plots of present samples are shown in Figures 2 through 4. The pyrene label concentration in these solutions ranges from 2.6 x 10^{-7} mol/L for ADPy-75

to 4.3 x 10^{-7} mol/L for ADPy-5 with the corresponding ionic monomer concentration of [AMPS] from 6.36 to 22.83 x 10^{-5} mol/L.

Figure 2 illustrates that quenching efficiency of Cu^{2+} increases with increasing charge density in the polymer and all data except that for ADPy-5 follow the curve bending downwards with increasing [Q]. There is only very weak quenching effect of Cu^{2+} for ADPy-5 with the lowest charge density.

Counterion condensation effect should be taken into account for interpreting the quenching of highly charged poly-electrolytes with cationic quenchers.[26]

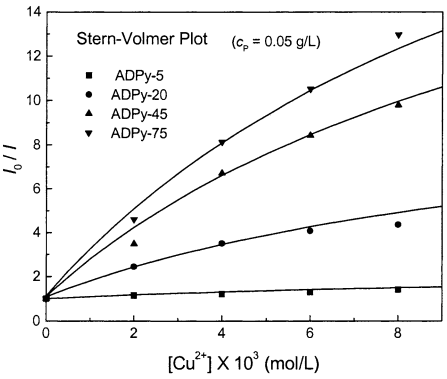

Figure 2. Fluorescence quenching by Cu^{2+} for pyrene labels on the samples with different AMPS contents in aqueous solutions. Curves: calculated from eq. 10.

The charge density parameter ξ is proportional to the AMPS mole fraction as[4]

$$\xi = F_{AMPS}\, q^2 / DkTb \qquad (3)$$

where q is the electronic charge in esu unit, D the dielectric constant of the solvent, k the Boltzmann constant, T the Kelvin temperature, and b the monomer length along the chain contour (usually b = 2.5 Å). Estimated ξ values of these samples are listed in Table 2. According to the Manning's modeling,[4] the criterion for divalent counterion Cu^{2+} to condense on polyanion is $\xi > 0.5$. Therefore, Cu^{2+} ions will condense on all samples of ADPy-20, ADPy-45, and ADPy-75, except ADPy-5. The condensed Cu^{2+} will induce the static quenching in addition to the dynamic quenching and the Stern-Volmer equation will be modified as the eq (2) of Ref. [26]

$$I_0 / I = (1 + K_{SV}[Cu^{2+}]_{eff}) \exp(n) \qquad (4)$$

Here, K_{SV} is the dynamic quenching constant, $[Cu^{2+}]_{eff}$ is the effective concentration of free Cu^{2+} ions which can actually quench the excited fluorophore by dynamic collisions since a large part of Cu^{2+} ions cannot be involved in quenching ultimately due to the $[Cu^{2+}]$ even two orders of magnitude higher than the [AMPS] in the present work. And n is the average number of condensed Cu^{2+} ions in one quenching effective sphere, given by

$$n = \alpha\, [Cu^{2+}]_{con} / [\text{pyrene}] \qquad (5)$$

where $[Cu^{2+}]_{con}$ is the concentration of condensed Cu^{2+} ions, [pyrene] is the concentration of pyrene residues, and α is the fraction of condensed Cu^{2+} ions existing in the quenching

effective sphere which quench the fluorophore with unity efficiency. For the our ADPy solutions, the total concentration $[AMPS]_0$ of AMPS unit is much lower than $[Cu^{2+}]$, so that the $[Cu^{2+}]_{con}$ for satisfying the condition of $\xi = 0.5$ will be evaluated from $[AMPS]_0$ as

$$[Cu^{2+}]_{con} = [AMPS]_0(1 - 1/2\xi) / 2 \qquad (6)$$

Condensation of counterion H^+ has been ignored because the condensation preferentially occurs for divalent counterion Cu^{2+}. Only very small part of free Cu^{2+} ions can collide with the excited fluorophore effectively due to the extremely low fluorophore content in the samples. By analogy to the Langmuir isothermal absorption,[27] the ζ fraction of fluorophores already quenched by free Cu^{2+} ions is

$$\zeta = K[Cu^{2+}]_{free} / (1 + K[Cu^{2+}]_{free}) \qquad (7)$$

So, $[Cu^{2+}]_{eff}$ is assumed to be proportional to the fluorophore unquenched

$$(1 - \zeta) / \zeta = [Cu^{2+}]_{eff} / \{[Cu^{2+}]_{free} - [Cu^{2+}]_{eff}\} \qquad (8)$$

$$[Cu^{2+}] = [Cu^{2+}]_{free} + [Cu^{2+}]_{con} \approx [Cu^{2+}]_{free} \qquad (9)$$

because $[Cu^{2+}]_{free} >> [Cu^{2+}]_{con}$. Here, K is the equilibrium constant for the free Cu^{2+} ion entering the counterion atmosphere surrounding the excited fluorophore by dynamic collision and $[Cu^{2+}]_{free}$ the free Cu^{2+} ion concentration. Substitute eqs (5)-(9) into eq (4),

$$I_0 / I = \{1 + K_{SV}[Cu^{2+}] / (1 + K[Cu^{2+}])\} \exp\{\alpha[AMPS]_0(1 - 1/2\xi) / 2[pyrene]\} \qquad (10)$$

The curves in Figure 2 are calculated results with the K_{SV}, K, and α values in Table 2 estimated by the best fitting. With increasing charge density of the samples, K_{SV} increases due to the increase in electrostatic attraction of the polyanion to the free cationic quencher Cu^{2+}. K reflects the equilibrium of Cu^{2+} ion entering and leaving the quenching effective atmosphere surrounding the fluorophore, consequently independent of the charge density. The α value is a probability product of a condensed Cu^{2+} ion encountering the nearest neighbor to the excited fluorophore and static quenching efficiency. The former is of millesimal owing to the mole ratio about $1.1\sim2.2 \times 10^{-3}$ for pyrene residue to AMPS unit in these samples and the 80% of pyrene more exposed to water easy to be accessed by the quencher as shown above. Therefore, the small α value estimated is reasonable, indicating that almost no change in static quenching occurs by increasing $[Cu^{2+}]$ in the observed $[Cu^{2+}]$ range because the counterion condensation is completed on the samples at the first Cu^{2+} concentration.

The upward bending of the curves in Stern-Volmer plot has been reported in some literature for cationic quenchers with the existence of anionic polyelectrolyte due to the increase in the static quenching,[23, 26, 28] since the quencher concentration is much lower than that required for condensation on the polyelectrolytes. However, the downward bending of the curves in

Figure 2 is based on the fact that addition of Cu^{2+} only increases $[Cu^{2+}]_{free}$, which in turn reduces the proportion of free Cu^{2+} ion effectively entering the counterion atmosphere surrounding the excited fluorophore.

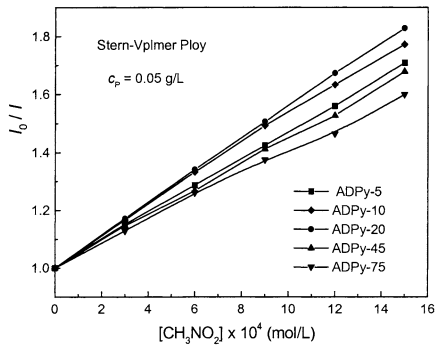

Figure 3. Fluorescence quenching by nitro-methane for pyrene labels on the samples with different AMPS contents in aqueous solutions.

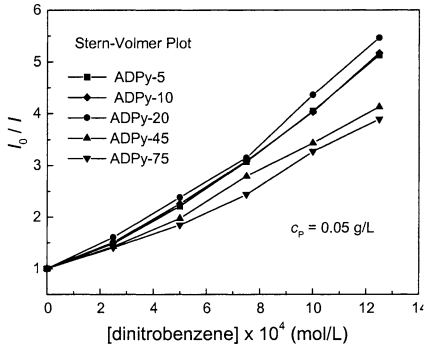

Figure 4. Fluorescence quenching by dinitro- benzene for pyrene labels on the samples with different AMPS contents in aqueous solutions.

As seen from Figures 3 and 4, the quenching efficiency of neutral quenchers nitromethane and dinitrobenzene does not change so much with the polymer charge density as the ionic quenchers. For easy comparison, we plotted the quenching rate constant k_q against F_{AMPS} in Figure 5. The curves for both quenchers are quite similar in shape, but the k_q value for dinitrobenzene is higher than that for nitromethane due to its higher hydro-phobicity and phenyl planar structure.

The F_{AMPS} dependence of the k_q in Figure 5 manifests the change in accessibility of the neutral quenchers to the pyrene label with the polymer charge density. When F_{AMPS} increases from 0.147 to 0.35, where no counterion condensation occurs for univalent H^+, the actual charge density is

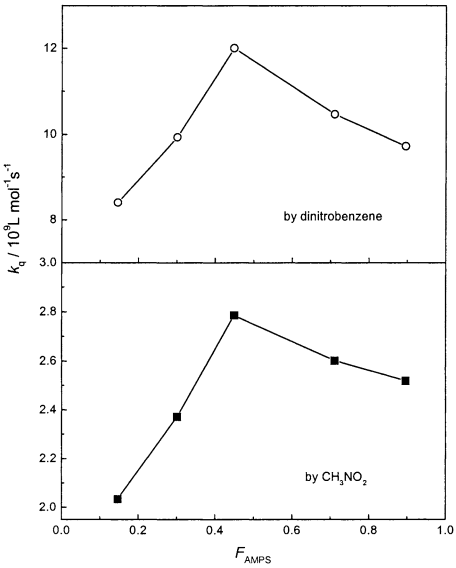

Figure 5. Plots of the quenching rate constant k_q for indicated quencher against the charge density F_{AMPS} of the sample.

increased monotonically. Consequently, the enhanced electrostatic repulsion between charged groups on the chain causes a more extended conformation. This effect, in turn, makes the fluorophore label be more easily approached by the quencher molecules. However, when the charge density exceeds 0.35, the counterion condensation occurs for univalent H^+ and the amount of condensed counterion increases with increasing charge density of the polymer. This appears to suggest that the decrease in k_q observed when F_{AMPS} exceeds 0.449 (for no sample of $F_{AMPS} = 0.365$ exactly) could be related to the counterion condensation.

Olea and Thomas[21] also found the decrease in the quenching rate constant k_q of molecular pyrene by nitromethane with increasing pH in aqueous solution of PMA when pH was higher than 9.0; they attributed this behavior to the deprotonation of nitromethane since their chromophore could be completely expelled into water in this pH range.

Relative Emission Intensity I_1/I_3

The relative emission intensity of the first peak to the third peak, I_1/I_3, of pyrene label on ADPy samples in water as well as in DMSO were plotted against F_{AMPS} in Figures 6 and 7, respectively. The data at the ordinate were obtained from the sample without ionic monomer AMPS. It is obvious that I_1/I_3 in water does decrease with increasing F_{AMPS}, especially it drops down abruptly at the F_{AMPS} interval from 0.449 (ADPy-20) to 0.574 (ADPy-30). Similar I_1/I_3 behavior in organic solvent DMSO means that this decrease is not due to the solvation difference for the copolymer backbone. At the same time, increasing polyelectrolyte

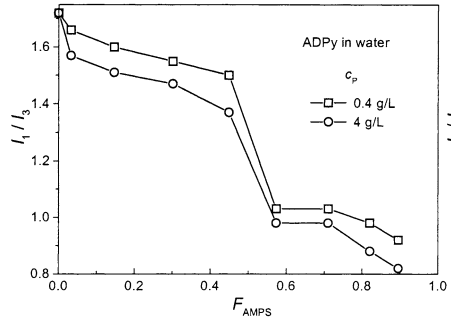

Figure 6. The relative emission intensity I_1/I_3 varies with mole fraction F_{AMPS} of AMPS in ADPy samples in salt-free aqueous solutions with indicated concentrations.

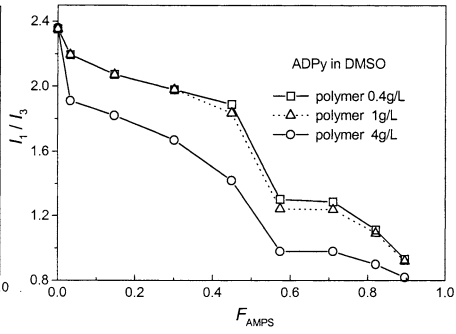

Figure 7. The relative emission intensity I_1/I_3 varies with mole fraction F_{AMPS} of AMPS in ADPy samples in DMSO solutions with indicated concentrations.

concentration also reduces the I_1/I_3 value, except for the sample without AMPS units.

According to the polarity scale function of I_1/I_3, the decrease in I_1/I_3 with increasing F_{AMPS} suggests that the pyrene label experiences a decreased polarity in its microenvironment with increasing charge density on its host chains. This less-polar environment may be originated from the local "temporal aggregated" domain of polyelectrolyte chains,[29] and the aggregation degree is enhanced by increasing charge density of polyelectrolytes. The pyrene groups labeled to the polyelectrolyte have no contribution to this aggregation because no excimer has been observed. This aggregation is not due to the hydrophobic association of the copolymer components either because both homopolymers of AMPS and DMAA are completely dissolvable in water as well as in DMSO. This finding contradicts the common understanding of polyelectrolytes.

Based on the classical theory for polyelectrolytes, the repulsive force is enhanced with increasing charge density, resulting in a more extended conformation for single chain or more segregated distribution for multi-chains in solution.[1, 2] Consequently, the labeled fluorophore is exposed further to the polar solvent with increasing charge density of the chain, this will cause an increase in I_1/I_3. As reported by Thomas group,[21, 25] poly(methacrylic acid) (PMA) chains take more extended conformation at pH > 6 and this makes I_1/I_3 of the pyrene label and probe abruptly increase.

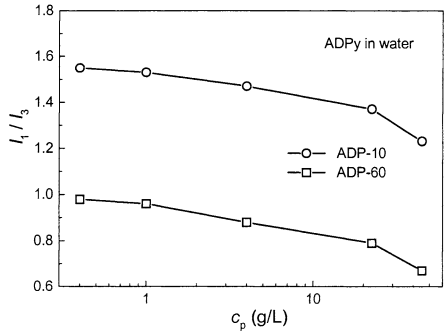

Figure 8. Polymer concentration c_P dependence of relative emission intensity I_1/I_3 of indicated samples in aqueous

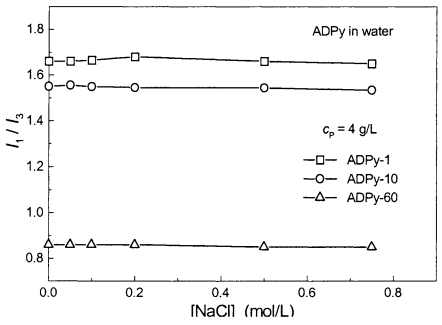

Figure 9. NaCl concentration dependence of relative emission intensity I_1/I_3 for indicated samples in aqueous solutions.

In order to revel the origin of this less-polar domain in dilute polyelectrolyte solutions, we determined polymer concentration c_P dependence of I_1/I_3 for two samples of ADPy-10 and ADPy-60 as shown in Figure 8. The gradual decrease in I_1/I_3 with increasing c_P indicates that

this less-polar domain is relevant to the amount of polyelectrolyte chains. In other words, the aggregation driving force would be resulted from the polyelectrolyte chain itself. This less-polar domain still exits in aqueous NaCl solution as illustrated in Figure 9, where I_1/I_3 for three ADPy samples is independent of salt concentration up to 0.75 mol/L and just takes the same value as in pure water, i.e., the less-polar domain cannot be destroyed with adding salt to screen the charge interaction. This fact means that once the less-polar domain is formed in polyelectrolyte solutions, the excessive energy is required to separate these chains again. Similar phenomenon has been observed in the volume phase transition of the polyelectrolyte gel with the same components occurring in DMSO/THF mixtures.[30,31] After the gel is shrunken by adding THF just beyond the threshold composition, excessive amount of DMSO, much more than the threshold, is needed to make the gel swell again to its original volume, manifesting the swelling hysteresis during the process.

Discussion

The above results, to authors' knowledge, firstly demonstrate the existence of the less-polar domain in aqueous as well as in polar organic solutions of polyelectrolytes. This domain is relevant to the polymer charge density and polyelectrolyte concentration but independent of the concentration of added salt. With the concept of "temporal aggregation" proposed by Bruno and Mattice,[29] these fluorescence phenomena can be interpreted consistently.

The temporal aggregation in polyelectrolyte solutions increases the local polymer concentration and decreases the accessibility of the fluorophore label surrounded by the chain backbone. The k_q value gives the averaged information for the pyrene labels in different environments while fluorescence decay data in Table 2 obviously show that after counterion condensation there appear two species of pyrene labels in two different environments. The existence of pyrene labels in the temporal aggregation domain with a slower decay rate induces the decrease in k_q with increasing charge density.

We try to predict the appearance of this less-polar aggregation domain in polyelectrolyte solutions in terms of counterion condensation. When charge density of polyelectrolyte chain exceeds the Manning's criterion of $\xi \geq 1$ for univalent counterion, the counterion will condense on the polyelectrolyte chain. The amount of counterions condensed on one charge site of polyelectrolyte is θ, and $\theta = 1 - 1/\xi$. Then, the total concentration c_b° of condensed counterion is

$$c_b^{\circ} = \theta F_{AMPS} c_P \qquad (11)$$

These condensed counterions will induce the aggregated dimmer of inter- or intra-polyelectrolyte chains as suggested by Bruno and Mattice.[29] Suppose that the condensed counterion outside the aggregation of concentration c_b is equilibrated with that in the aggregated dimmer cluster of concentration c_D, then

$$K_D = c_D / c_b^2 \qquad (12)$$

$$c_b = c_b^o - 2c_D \qquad (13)$$

Here, K_D is equilibrium constant for this "temporal aggregating" reaction and can be evaluated from the free energy ΔG. Ray and Manning have estimated the free energy for two infinitely long parallel linear polyelectrolytes and found attractive interaction when the distance between two polyelectrolytes is inside a Debye radius intermediately.[5-8] Because the counterion concentration in present aqueous solutions of about 2 x 10^{-3} mol/L (so that Debye radius κ^{-1} = 96 Å) is close to that used in Ray and Manning's simulation,[5] we adopt their free energy value of -1.25 kcal/mol at the minimum to calculate K_D value as 8.62 L/mol since the separation distance about 50 Å at the minimum is in consistent with the Förster transfer radius at which "temporal aggregates" were observed by Bruno and Mattice.[29]

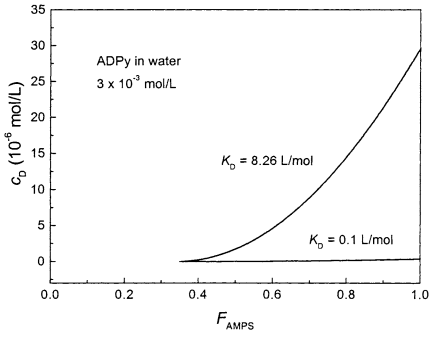

Figure 10. Calculated "temporal aggregated" dimmer concentration c_D plotted against mole fraction F_{AMPS} of AMPS in ADPy samples with indicated equilibrium constant K_D.

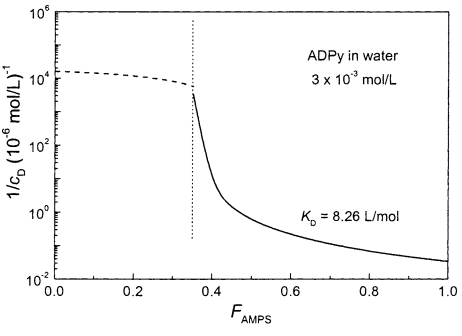

Figure 11. Reciprocal of calculated c_D (solid line) with dashed line guiding eyes for samples without counterion condensation, analogy to those in Figures 6 and 7.

Figure 10 depicts calculated c_D of the aggregated dimmer varying with F_{AMPS} for the ADPy samples of 3 x 10^{-3} mol/L. At K_D = 8.62 L/mol, c_D is greatly increased with F_{AMPS} after the counterion condensation occurs at F_{AMPS} > 0.35 but its highest value is less than 1% of c_b^o. However, if the K_D is small (saying 0.1 L/mol) there are almost no aggregated clusters.

It is difficult to formulate I_1/I_3 with "temporal aggregated" dimmer concentration c_D directly.

However, following the idea suggested by Khokhlov and Kramarenko in their simulation for the volume phase transition in polyelectrolyte gels,[32] the effective dielectric constant is composed of those of the solvent and polymer and the polarity of a polyelectrolyte backbone is much lower. Therefore, the formation of "temporal aggregated" dimmers increases the local polymer concentration and reduces the polarity of the microenvironment. We plotted the reciprocal of c_D against F_{AMPS} in Figure 11 by solid line with a dash line guiding eyes for the samples without counterion condensation. The change of I_1/I_3 with F_{AMPS} is reasonably reproduced by the simulation, indicating that the decrease in I_1/I_3 is caused by the "temporal aggregates" in polyelectrolyte solutions due to the attractive potential to the condensed counterions.

Acknowledgment

We are grateful to the NNSF of China (No. 29725411) and the NSF of Guangdong Province (No. 015036) for the financial support to this work.

[1] C. Tanford, "*Physical Chemistry of Macromolecules*", John Wiley & Sons, New York 1961, p. 457.
[2] H. Dautzenberg, W. Jaeger, J. Kötz, B. Philipp, C. Seidel, D. Stscherbina, "*Polyelectrolytes*", Hanser, Munich 1994, p.87.
[3] F. Oosawa, "*Polyelectrolytes*", Marcel Dekker, New York 1971, p. 23.
[4] G. S. Manning, in: "*Polyelectrolytes*", E. Selegny, Eds., Reidal Publisher, Dordrecht, Holland 1974, p. 9.
[5] J. Ray, G. S. Manning, *Langmuir* **1994**, *10*, 2450.
[6] J. Ray, G. S. Manning, *Macromolecules* **1997**, *30*, 5739.
[7] J. Ray, G. S. Manning, *Macromolecules* **1999**, *32*, 4588.
[8] J. Ray, G. S. Manning, *Macromolecules* **2000**, *33*, 2901.
[9] J. Bodycomb, M. Hara, *Macromolecules* **1995**, *28*, 8190.
[10] B. D. Ermi, E. J. Amis, *Macromolecules* **1996**, *29*, 2701.
[11] M. Sedlák, *J. Chem. Phys.* **1996**, *105*, 10123.
[12] R. Borsali, H. Nguyen, R. Pecora, *Macromolecules* **1998**, *31*, 1548.
[13] H. Matsuoka, Y. Ogura, H. Yamaoka, *J. Chem. Phys.* **1998**, *109*, 6125.
[14] H. Liu, L. Skibinska, J. Gapinski, A. Patkowski, E. W. Fischer, R. Pecora, *J. Chem. Phys.* **1998**, *109*, 7556.
[15] L. Skibinska, J. Gapinski, H. Liu, A. Patkowski, E. W. Fischer, R. Pecora, *J. Chem. Phys.* **1999**, *110*, 1794.
[16] B. D. Ermi, E. J. Amis, *Macromolecules* **1997**, *30*, 6937.
[17] Y. Morishima, *Prog. Polym. Sci.* **1990**, *15*, 949.
[18] M. A. Winnik, "*Photophysical and Photochemical Tools in Polymer Science*", Reidel, Dordrecht, Holland 1986, p. 15.
[19] F. Gao, Y. Yan, B. Ren, Z. Tong, *Chem. J. Chinese U.* (in Chinese) **2000**, *21*, 976.
[20] Y. Morishima, Y. Tominaga, M. Kamachi, T. Okada, Y. Hirata, N. Mataga, *J. Phys. Chem.* **1991**, *95*, 6027.
[21] A. F. Olea, J. K. Thomas, *Macromolecules* **1989**, *22*, 1165.
[22] C. E. Hoyle, P. W. Neilson, P. M. Chatterton, M. A. Trapp, *Macromolecules* **1991**, *24*, 2194.
[23] H. Yamamoto, M. Mizusaki, K. Yoda, Y. Morishima, *Macromolecules* **1998**, *31*, 3588.
[24] M. Suwa, A. Hashidzume, Y. Morishima, T. Nakato, M. Tomida, *Macromolecules* **2000**, *33*, 7884.
[25] D.-Y. Chu, J. K. Thomas, *Macromolecules* **1984**, *17*, 2142.
[26] Y. Morishima, H. Ohgi, M. Kamachi, *Macromolecules* **1993**, *26*, 4293.
[27] G. M. Barrow, "*Physical Chemistry*", 4th ed., McGraw-Hill, London 1979, p.
[28] J. A. Delaire, M. A. J. Rodgers, S. E. Webber, *J. Phys. Chem.* **1984**, *88*, 6219.

[29] K. R. Bruno, W. L. Mattice, *Macromolecules* **1992**, *25*, 327.
[30] X. Liu, Z. Tong, X. Cao, O. Hu, *Polymer* **1996**, *37*, 5947.
[31] X. Liu, Z. Tong, F. Gao, *Polym. Intern.* **1998**, *47*, 215.
[32] R. Khokhlov, E. Yu. Kramarenko, *Macromol. Theory. Simul.* **1994**, *3*, 4537.